

Supplementary Materials for
**Loss of histone macroH2A1.1 causes kidney abnormalities secondary to a
change in nutrient metabolism**

René Winkler *et al.*

Corresponding author: Marcus Buschbeck, mbuschbeck@carrerasresearch.org;
Raffaele Teperino, raffaele.teperino@helmholtz-munich.de;
Martin Hrabě de Angelis, martin.hrabedeangelis@helmholtz-munich.de

Sci. Adv. **11**, eadz1242 (2025)
DOI: 10.1126/sciadv.adz1242

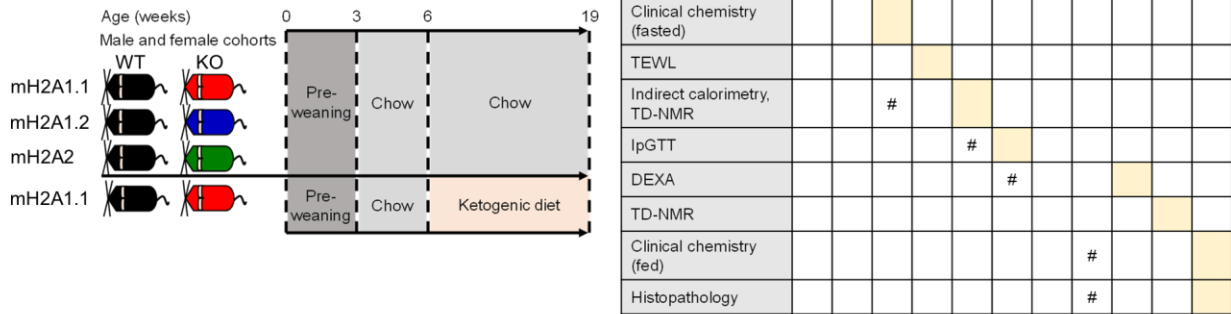
The PDF file includes:

Figs. S1 to S8
Tables S1, S3, and S4
Extended Data E1
Legends for tables S2, S5, and S6

Other Supplementary Material for this manuscript includes the following:

Tables S2, S5, and S6

A



B

Sex-independent histopathologic findings

Organ	mH2A1.1 KO	mH2A1.2 KO	mH2A2 KO	mH2A1.1 KO under KD*
Adrenal glands	No	No	No	No
Blood vessels	No	No	No	No
Brain/Cerebellum	No	No	No	No
Cartilages	No	No	No	No
Colon	No	No	No	No
Duodenum/Jejunum	No	No	No	No
Esophagus	No	No	No	No
Heart	No	No	No	No
Kidneys	Yes 1)	4)	No	No
Liver	No	5)	No	No
Lung	No	No	No	No
Lymph nodes	No	No	No	No
Pancreas	No	No	No	No
Parathyroid	No	No	No	No
Rectum	No	No	No	No
Salivary glands	No	No	No	No
Skeletal muscle	No	No	No	No
Skin	No	No	No	No
Spleen	No	No	No	No
Stomach	2)	No	No	No
Thymus	No	6)	No	No
Thyroid	No	No	No	No
Trachea	No	No	No	No
Urinary bladder	No	No	No	No
WAT/BAT	3)	No	No	No

1) Renal infarct, interstitial inflammatory infiltrates, and intratubular hyaline casts as described in Figure 1.

2) Female mH2A1.1 KO only: Forestomach ulceration in 40% and hyperplasia in 40% of analyzed mice.

3) Male mH2A1.1 KO only: Focal whitening of BAT in 40% of analyzed mice.

4) Intratubular hyaline casts were only enriched in female mH2A1.2 KO mice.

5) Female mH2A1.2 KO only: Hepatitis in 20%, micro-/macrosteatosis in 20%, and immune infiltrates in 20% of mice.

6) Male mH2A1.2 KO only: Thymic cysts in 50% of analyzed mice.

* No differences compared to WT under KD. KD-dependent effects were present, such as liver steatosis.

Fig. S1. Phenotypic screening and histopathologic results (accompanying Fig. 1).

(A) Outline of the highly standardized screen. Indicated tests were performed at the depicted age. # indicates tests that were performed for macroH2A2 KO mice and control littermates at an earlier

time point. TEWL, Trans-epidermal water loss; TD-NMR, Time Domain Nuclear Magnetic Resonance; IpGTT, intraperitoneal glucose tolerance test; DEXA, Dual-Energy X-ray Absorptiometry.

(B) Overview of sex-independent histopathologic findings across 25 organs in isoform-specific knock-out mouse models of histone variants. KD, ketogenic diet.

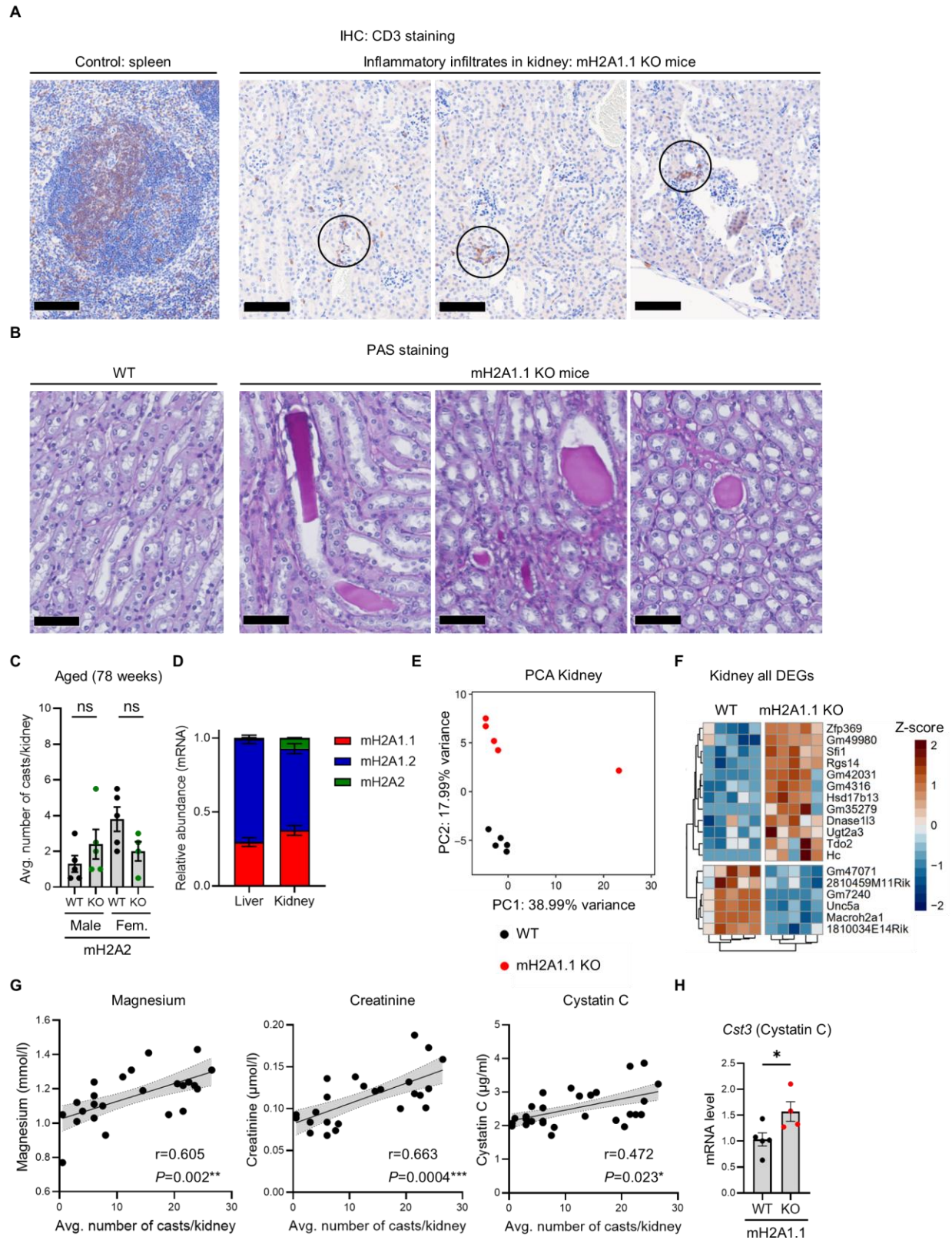


Fig. S2. Histological and transcriptional analyses of macroH2A1.1 KO kidneys (accompanying Fig. 1).

- (A) Immunohistochemistry (IHC) staining of CD3-positive cells (T cells) for kidneys with confirmed inflammatory infiltrates. Circles show accumulation of T cells. The bar indicates 50 μ m.
- (B) PAS (periodic acid-Schiff) staining of detected kidney casts. Positive PAS reaction suggests that glycosylated proteins form the observed casts, such as Uromodulin/Tamm-Horsfall protein. The bar indicates 50 μ m.
- (C) Average number of kidney casts per kidney in a cohort of aged macroH2A2 KO mice (78 weeks old). Data are displayed as mean \pm SEM. ns, not significant, calculated by Two-way ANOVA with Fisher's LSD.
- (D) Relative mRNA abundance was compared between macroH2A variants in liver and kidney tissue from WT mice. Values were calculated in relation to the housekeeping genes *Gapdh* and *Rplp0*. Data are compiled from Fig. 1H and Fig. 3C.
- (E) Principal Component Analysis (PCA) plot of the kidney samples from the RNA-Seq in Fig. 1I using the top 100 most variable genes is shown. Removal of the most variant KO sample did not affect the low number of differentially expressed genes (DEGs).
- (F) A heatmap of all DEGs from Fig. 1I and individual expression among samples is shown (Z-score scaled values by mean subtraction and division by the standard deviation).
- (G) Correlation of average number of kidney casts per kidney in mice that were between 30 and 76 weeks old with typical indicators of kidney disease. No discrimination between genotypes was made. Magnesium, creatinine, and Cystatin C levels were measured in peripheral blood. Linear regression was performed and is shown with 90% confidence interval. Pearson's correlation coefficient (r) is displayed with significance. Only mice up to an average of 26.5 casts per kidney were included to reflect gradual increase.
- (H) The relative levels of mRNA encoding the kidney damage marker Cystatin C. Data are displayed as mean \pm SEM. P -value was calculated with an unpaired Student's t -test. *, $P < 0.05$.

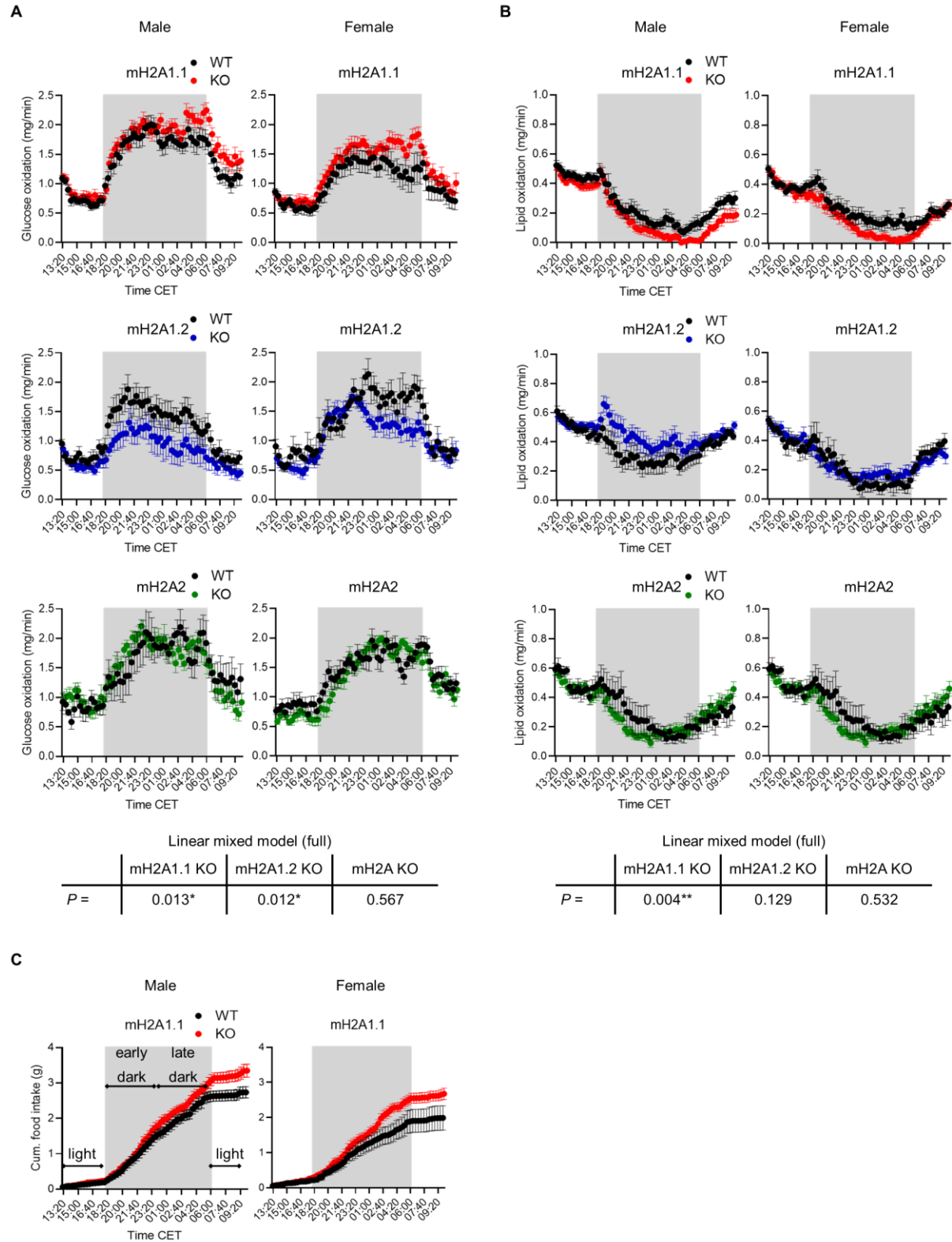


Fig. S3. Glucose and lipid oxidation rates (accompanying Fig. 2).

(A) Glucose and (B) lipid oxidation rates were determined for 21 h every 20 min for young adult WT and age-matched macroH2A (mH2A) isoform-deficient (KO) mice of both sexes ($n=5-15$ per

group). The nighttime is indicated in grey. Data are plotted as mean \pm SEM. A full linear mixed model by Restricted Maximum Likelihood was calculated and likelihood ratio test Chi-square is given as *P*.

(C) Cumulative food intake is shown for male and female mice with macroH2A1.1 wild-type or knock-out. Data are plotted as mean \pm SEM.

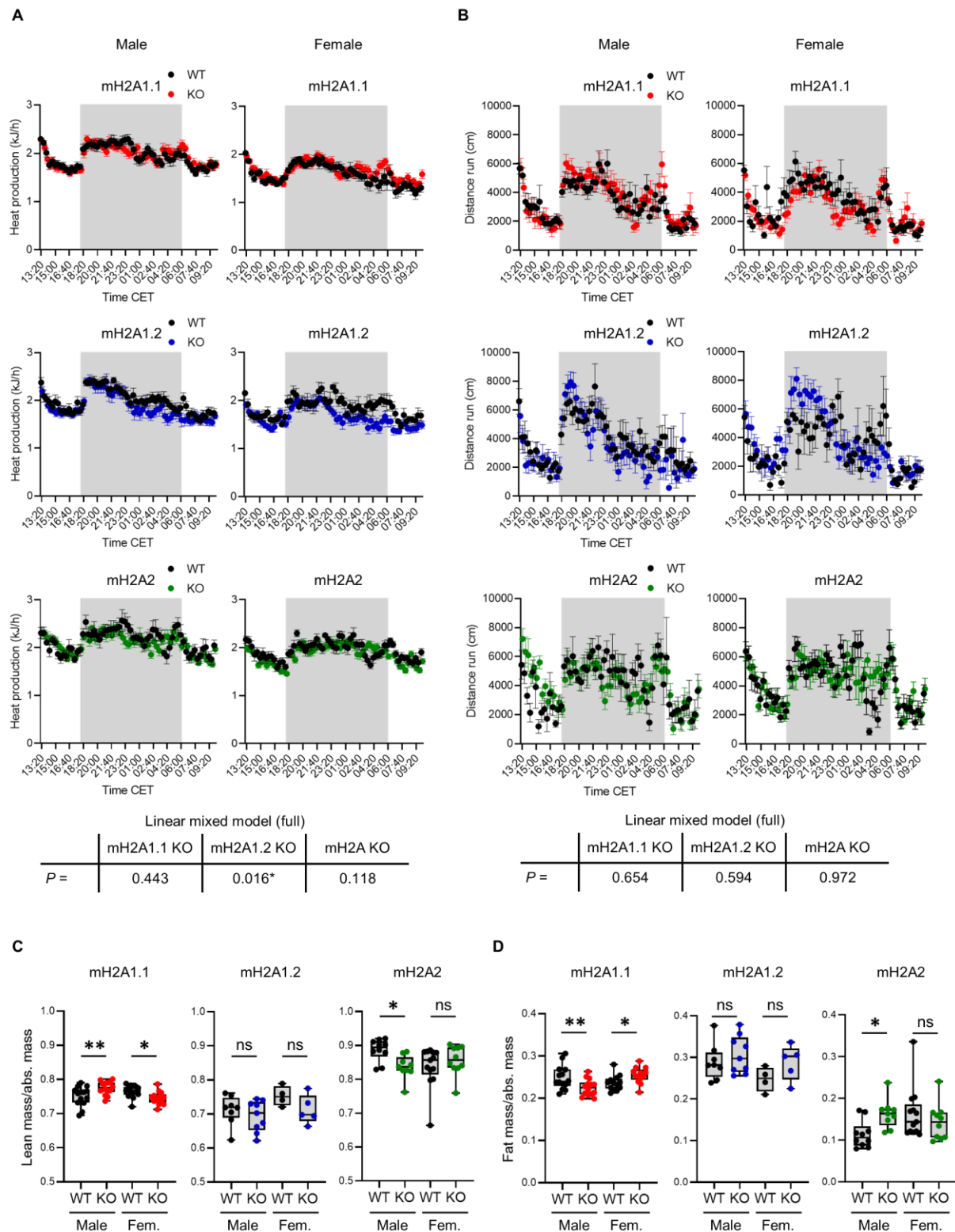


Fig. S4. MacroH2A1.1-deficient mice have unaltered heat production and activity (accompanying Fig. 2).

(A) Heat production and (B) locomotor activity based on distance run were recorded. Outlier exclusion was performed using ROUT's algorithm ($Q=0.1\%$). A full linear mixed model by Restricted Maximum Likelihood was calculated and likelihood ratio test Chi-square is given as P . (C) Relative lean and (D) fat mass was assessed of isoform-specific macroH2A KO and control littermates by Time Domain Nuclear Magnetic Resonance (TD-NMR; macroH2A1.1 and macroH2A1.2 KO) or Dual-Energy X-ray Absorptiometry scan (DEXA; macroH2A2 KO) and normalized to absolute mass. Each dot represents an individual animal. Boxes display Q1 and Q3, the median as a band, and minimum to maximum range. P -values were calculated by Two-way ANOVA with Fisher's LSD. *, $P<0.05$; **, $P<0.01$; ns, not significant.

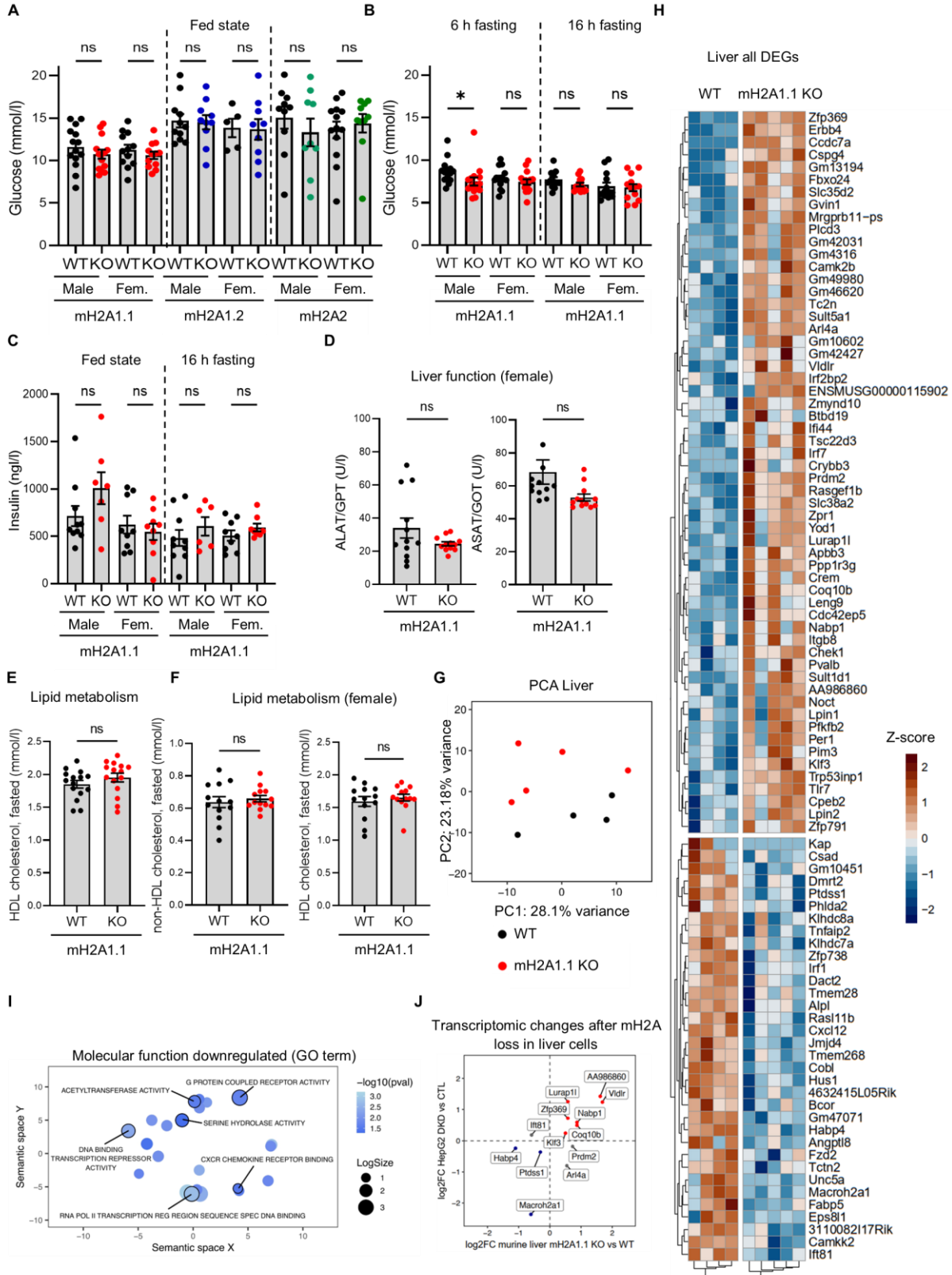


Fig. S5. Sex-specific effects on glucose metabolism and hepatic gene expression after macroH2A1.1 depletion (accompanying Fig. 3).

(A) Steady-state glucose levels were measured in plasma from peripheral blood of fed mice of the indicated genotypes and sex ($n \geq 5$ per group) under a standard chow diet. Data are plotted as mean \pm SEM. *P*-values were calculated by Two-way ANOVA with Fisher's LSD. ns, not significant.

(B) Fasted glucose levels were measured in plasma from peripheral blood of WT or macroH2A1.1 KO ($n \geq 13$ per group). Data are plotted as in (A). *P*-values were calculated by Two-way ANOVA with Fisher's LSD. *, $P < 0.05$; ns, not significant.

(C) Insulin levels were measured in plasma from peripheral blood of an aged cohort of sex- and age-matched WT and macroH2A1.1 KO mice ($n \geq 6$ per group). Measurements were taken in a fed state or after 16 h of starvation. Data are plotted as in (A). *P*-values were calculated by Two-way ANOVA with Fisher's LSD. ns, not significant.

(D) Parameters of liver function were compared in plasma from peripheral blood of female macroH2A1.1 KO mice and control WT littermates under standard diet conditions ($n=12$ per group): alanine aminotransferase/glutamate pyruvate transaminase (ALAT/GPT) and aspartate aminotransferase/glutamic oxaloacetic transaminase (ASAT/GOT) activity. Data is plotted as mean \pm SEM. Unpaired Student's *t*-test with Welch's correction, if needed. ns, not significant.

(E) High-density-lipoprotein (HDL) cholesterol levels were measured in the plasma of fasted male WT or macroH2A1.1 KO mice ($n=15$ per group). Data are displayed and statistics were performed as in Fig. 3E. ns, not significant.

(F) Non-HDL cholesterol levels, calculated from total cholesterol minus HDL cholesterol, and HDL cholesterol levels, measured in the plasma of female fasted WT or macroH2A1.1 KO mice ($n=13$ per group), are shown. Data are displayed and statistics were performed as in Fig. 3E. ns, not significant.

(G) Principal Component Analysis (PCA) plot of the liver samples from RNA-Seq in Fig. 3F using the top 100 most variable genes.

(H) A heatmap of all DEGs from Fig. 3F and individual expression among samples (Z-score scaled values by mean subtraction and division by the standard deviation).

(I) Gene Ontology (GO) analysis was performed on the complete data set from Fig. 3F. Significantly downregulated GO terms of molecular functions ($P < 0.05$) were clustered using the Revigo tool. REG, regulatory.

(J) DEGs from Fig. 3F were overlapped with DEGs from a data set of human HepG2 liver cells with knock-out of all macroH2A isoforms (DKD). Red indicates commonly upregulated and blue commonly downregulated genes after macroH2A loss.

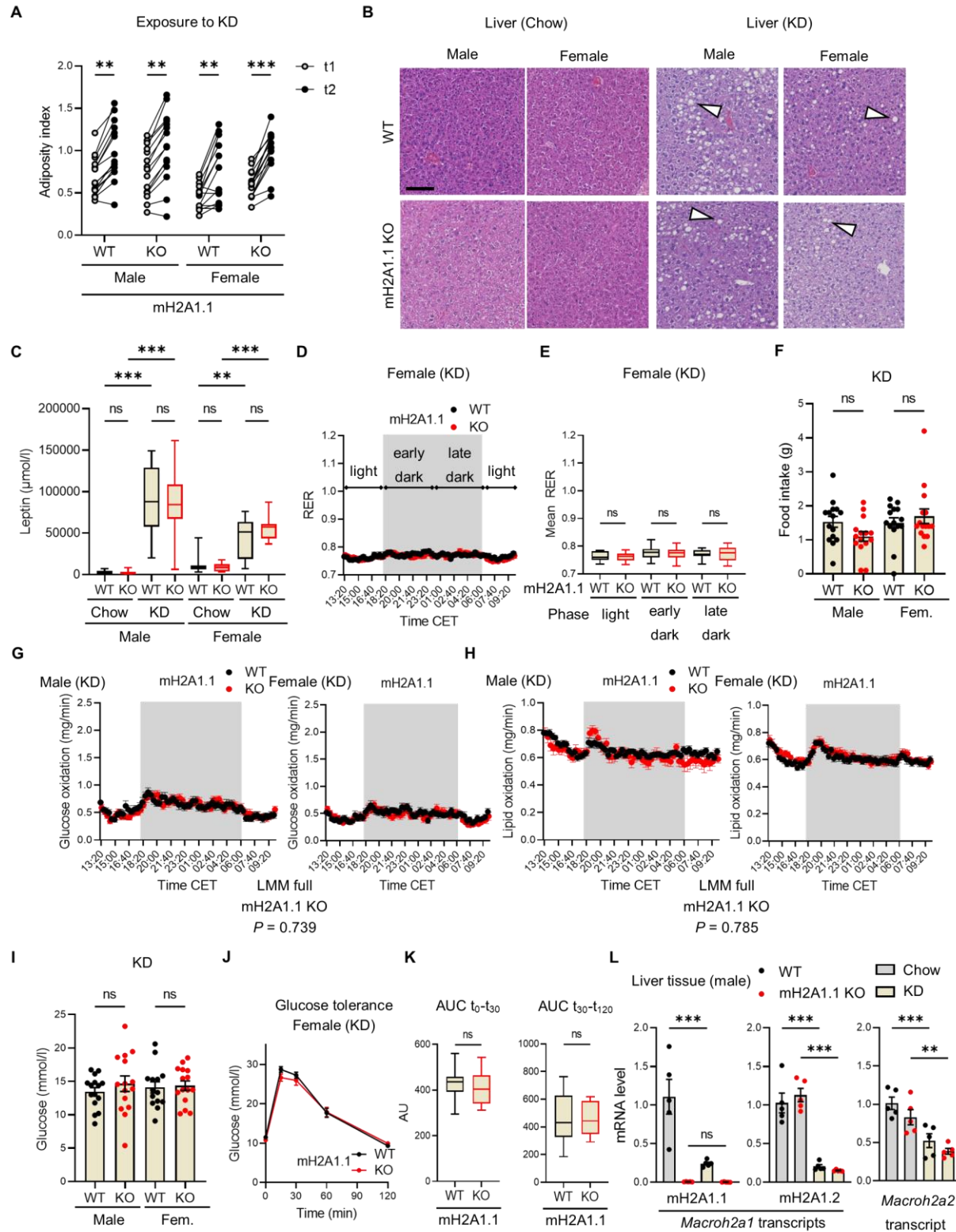


Fig. S6. Effects of ketogenic diet on WT and macroH2A1.1 KO mice (accompanying Fig. 4).

(A) Male and female macroH2A1.1 KO mice and control WT littermates were fed a ketogenic diet (KD) for 13 weeks starting at the age of 6 weeks. The adiposity index was calculated as the ratio

of fat mass to lean mass from two different time points (t1=age of 13 weeks and t2=age of 18 weeks). *P*-values were calculated using Two-way-ANOVA. **, *P*<0.01; ***, *P*<0.001.

(B) H&E-stained sections of the liver showed pronounced steatosis under KD conditions. The bar indicates 100 μ m.

(C) Steady-state leptin levels were measured in plasma from peripheral blood of male and female mice fed chow or KD of the indicated genotypes (*n*≥10 per group). Boxes display Q1 and Q3, the median as a band, and minimum to maximum range. *P*-values were calculated by Welch's ANOVA with Dunnett's T3 correction. **, *P*<0.01; ***, *P*<0.001; ns, not significant.

(D) Respiratory exchange rates (RER) were measured and plotted as in Fig. 4A for female macroH2A1.1 KO mice and control WT littermates under KD (*n*=15 per group).

(E) Comparison of the mean RER between female WT or macroH2A1.1 KO mice under KD of three different phases: light (13:00–18:00 CET, 6:00–10:00 CET), early dark (18:00–0:00 CET), and late dark (0:00–6:00 CET) based on the data shown in (D). Boxes display Q1 and Q3, the median as a band, and minimum to maximum range. *P*-values were calculated by Two-way ANOVA with Fisher's LSD. ns, not significant.

(F) Food intake was tracked during RER measurements for each mouse under KD within 21 h. Data are displayed as mean \pm SEM. Each dot indicates one individual mouse. *P*-values were calculated by Two-way ANOVA with Fisher's LSD. ns, not significant.

(G) Glucose and **(H)** lipid oxidation rates were determined for 21 h every 20 min for young adult WT and age-matched macroH2A1.1 (mH2A1.1) isoform-deficient (KO) mice of both sexes (*n*=15 per group). The nighttime is indicated in grey. Data is plotted as mean \pm SEM.

(I) Steady-state glucose levels were measured in plasma from peripheral blood of fed male and female mice of the indicated genotypes under KD (*n*≥14 per group). Data are displayed as mean \pm SEM. *P*-values were calculated by Two-way ANOVA with Fisher's LSD. ns, not significant.

(J) An intraperitoneal glucose tolerance test was performed and displayed as in Fig. 4A for female mice of the indicated genotypes under KD (*n*=15 per group).

(K) The area under the curve (AUC) was calculated and plotted as in Fig. 4D. Unpaired Student's *t*-test. ns, not significant.

(L) Gene expression of genes encoding macroH2A variants was measured by RT-qPCR in whole liver tissue from male mice of both genotypes (*n*=5 per group) under the indicated diet conditions. Fold induction was normalized to the mean of the corresponding WT samples. Data are displayed as mean \pm SEM. *P*-values were calculated using One-way-ANOVA with Fisher's LSD. **, *P*<0.01; ***, *P*<0.001; ns, not significant.

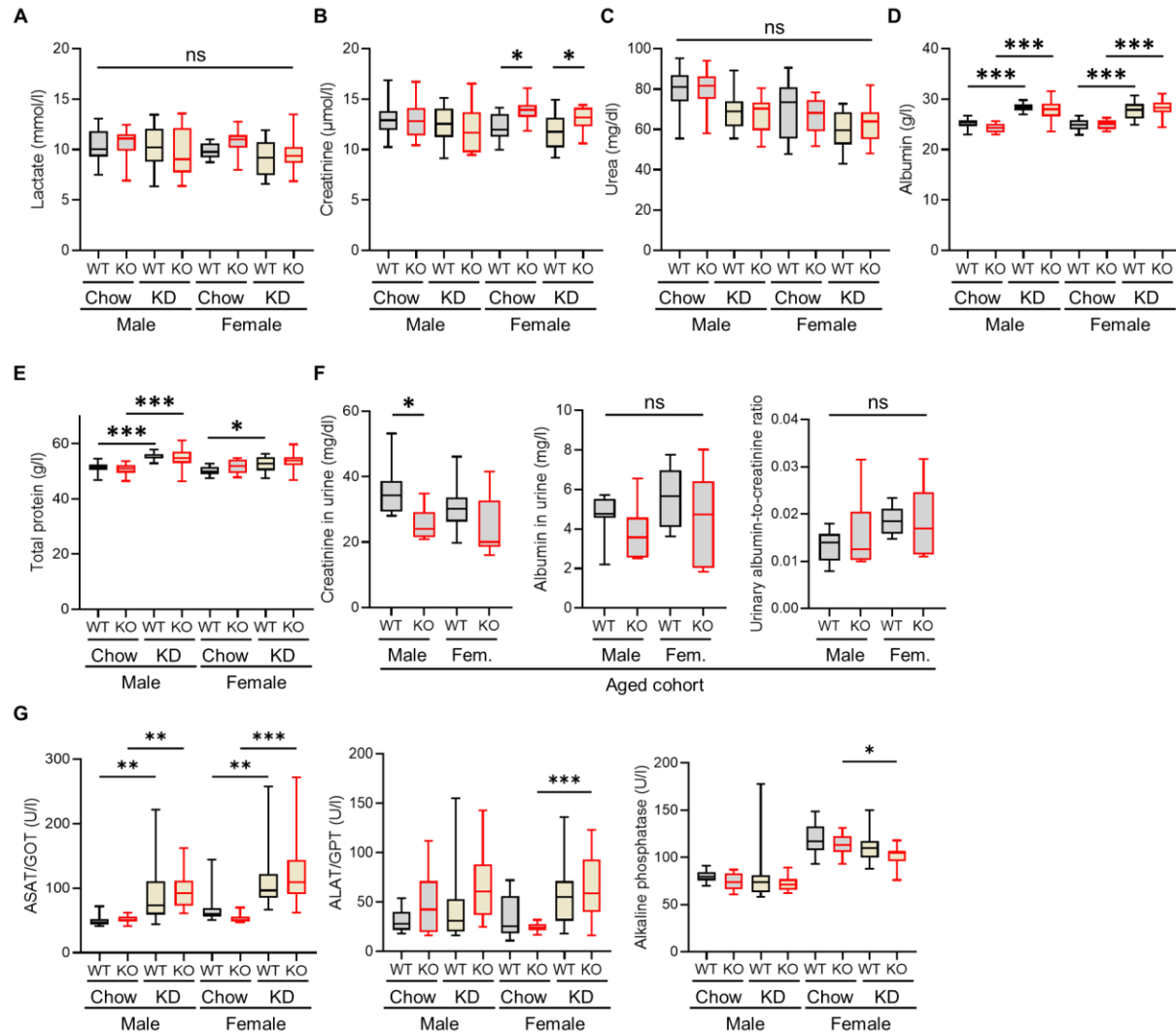


Fig. S7. Clinical chemistry of WT and macroH2A1.1 KO mice under chow or ketogenic diet. (accompanying Fig. 5)

(A) Lactate, (B) creatinine, (C) urea, (D) albumin, and (E) total protein levels were measured in peripheral blood of fed WT or macroH2A1.1 KO mice ($n \geq 12$ per group). Boxes display Q1 and Q3, the median as a band, and minimum to maximum range. P -values were calculated by Three-way ANOVA with Welch's correction. *, $P < 0.05$; ***, $P < 0.001$; ns, not significant. KD, ketogenic diet.

(F) Urinary creatinine and urinary albumin levels were measured in fed WT or macroH2A1.1 KO mice ($n \geq 5$ per group, aged cohort of sex- and age-matched mice). Urinary albumin-to-creatinine ratio was calculated. Data are displayed as in (A). P -values were calculated by Two-way ANOVA with Fisher's LSD. *, $P < 0.05$.

(G) Alanine aminotransferase/glutamate pyruvate transaminase (ALAT/GPT), aspartate aminotransferase/glutamic oxaloacetic transaminase (ASAT/GOT), and alkaline phosphatase activity were measured in peripheral blood of fed WT or macroH2A1.1 KO mice ($n \geq 12$ per group). Data for mice on chow diet are also shown in Fig. 3D and S5D. P -value was calculated by Three-way ANOVA with Fisher's LSD. *, $P < 0.05$; **, $P < 0.01$; ***, $P < 0.001$; ns, not significant. KD, ketogenic diet.

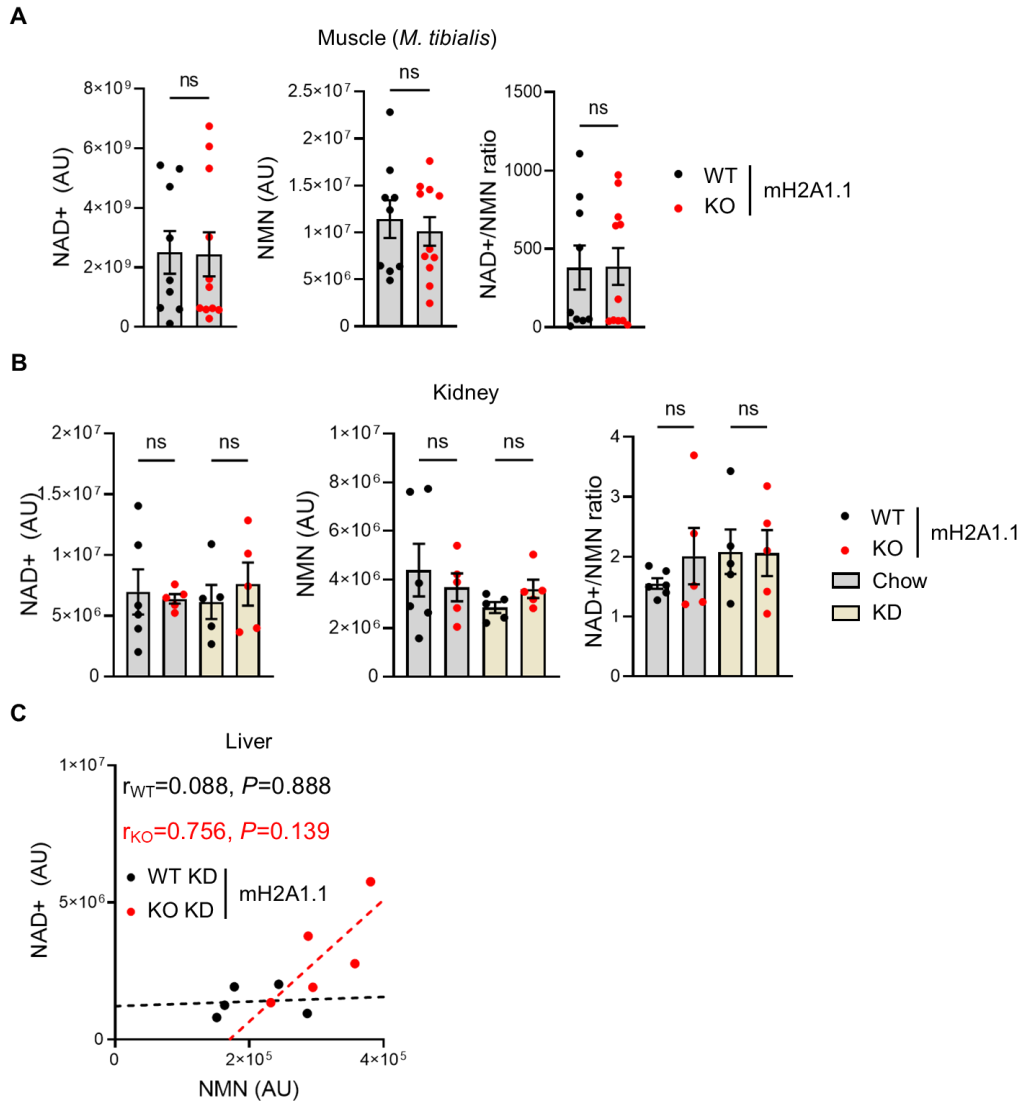


Fig. S8. Targeted metabolomics of tissues from WT and macroH2A1.1 KO mice under chow or ketogenic diet. (accompanying Fig. 6)

(A) NAD⁺ and NMN levels were measured by a targeted metabolomics approach in muscle tissue from male WT or macroH2A1.1 (mH2A1.1) KO mice that received a standard chow diet. The NAD⁺/NMN ratio was calculated. Data are displayed as mean \pm SEM. Each dot indicates one individual mouse. Student's *t*-test. ns, not significant.

(B) NAD⁺ and NMN levels were measured by a targeted metabolomics approach in kidney tissue from male WT or macroH2A1.1 KO mice that received a standard chow or ketogenic diet. The NAD⁺/NMN ratio was calculated. Data are displayed as mean \pm SEM. Each dot indicates one individual mouse. Two-way ANOVA with Fisher's LSD. ns, not significant.

(C) NAD⁺ and NMN levels were measured by a targeted metabolomics approach in liver tissue from male WT or macroH2A1.1 KO mice that received a ketogenic diet. Correlation of NMN and NAD⁺ levels was performed and linear regression line inserted. Pearson's correlation coefficient (*r*) is displayed with significance.

Table S1. Overview of analyzed mouse cohorts besides the phenotyping cohorts shown in fig. S1A. Genotype, background, sex, diet, age at analysis, and the corresponding Fig. where the data were used are listed. WT, wild-type; mH2A, macroH2A; M, male; F, female.

Genotype	Background	Sex	Diet	Age (weeks)	Analysis	Figure
WT / mH2A1.1 KO	C57BL/6J	M	Chow / Ketogenic Diet	17	RNA-seq, RT-qPCR, targeted metabolomics	1H–J, 3C, 3F, 3G, 4E, 6A–C, S2D, S2E, S2F, S2H, S5G, S5H, S8A–C
WT / mH2A1.1 KO	C57BL/6 (predominant) X SV129	F/M	Chow	16	Histopathology	1E
WT / mH2A1.2KO+mH2A2 KO	C57BL/6 X SV129	F/M	Chow	21	Histopathology	1G
WT m / H2A1.1 KO WT / mH2A1.2 KO	C57BL/6J	F/M	Chow	30-76	Urine collection, clinical chemistry (fed and fasted), histopathology	1F, S2G, S5C, S7F
WT / mH2A2 KO	C57BL/6J	F/M	Chow	78	Histopathology	S2C

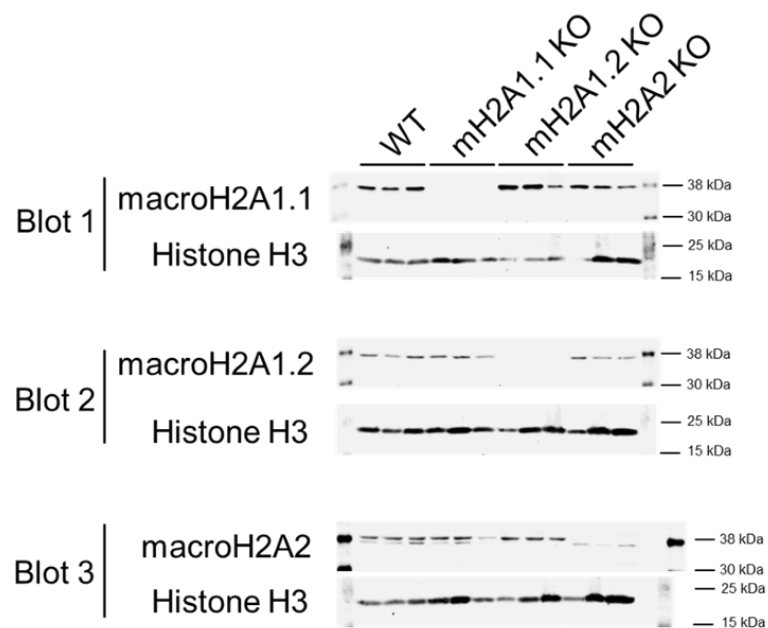
Table S3. Correlation of clinical chemistry parameters and average cast count per kidney (accompanying fig. S2). Correlation of average number of kidney casts per kidney in mice that were between 30 and 76 weeks old with clinical chemistry measurements from peripheral blood and urine. No discrimination between genotypes was made. Pearson's correlation coefficient (r) is displayed with significance. Only mice up to an average of 26.5 casts per kidney were included. ALAT/GPT, alanine aminotransferase/glutamate pyruvate transaminase; ASAT/GOT, aspartate aminotransferase/glutamic oxaloacetic transaminase; BHB, beta-hydroxybutyrate; HDL, high-density lipoprotein; NEFA, non-esterified fatty acids; uACR, urinary albumin-to-creatinine ratio; UIBC, unsaturated iron-binding capacity.

Parameter	r	P		Parameter	r	P	
Albumin	-0.309	0.142	ns	Lactate	-0.011	0.959	ns
ALAT/GPT	0.029	0.893	ns	Magnesium	0.605	0.002	**
Alkaline Phosphatase	-0.102	0.637	ns	NEFA	0.053	0.839	ns
alpha-Amylase	-0.038	0.859	ns	Phosphate	0.508	0.092	ns
ASAT/GOT	0.195	0.361	ns	Potassium	0.236	0.267	ns
BHB	-0.107	0.716	ns	Sodium	0.051	0.814	ns
Bilirubin (total)	-0.101	0.647	ns	Total bile acids	0.221	0.411	ns
Calcium	0.225	0.291	ns	Total protein	-0.281	0.206	ns
Chloride	0.226	0.289	ns	Triglycerides	0.191	0.408	ns
Cholesterol	-0.145	0.732	ns	uACR	0.136	0.628	ns
Creatinine	0.663	0.0004	***	UIBC	0.403	0.063	ns
Cystatin C	0.472	0.023	*	Urea	-0.228	0.32	ns
Glucose	-0.511	0.011	*	Urinary albumin	-0.219	0.434	ns
Glycerol	0.253	0.345	ns	Urinary creatinine	-0.598	0.011	*
HDL-cholesterol	-0.309	0.141	ns	Urinary KIM1	-0.141	0.533	ns
Iron (total)	0.074	0.731	ns				

Table S4. A full linear mixed model by Restricted Maximum Likelihood for RER measurements. Statistical parameters for indicated comparisons are given.

macroH2A1.1 KO versus WT								
Effect	group	term	estimate	std.error	statistic			
fixed	NA	(Intercept)	0.876	0.012	71.764			
fixed	NA	genotypemutant	0.033	0.011	2.914			
fixed	NA	sexm	0.017	0.011	1.520			
random	timepoint	sd__(Intercept)	0.055	NA	NA			
random	identifier	sd__(Intercept)	0.042	NA	NA			
random	Residual	sd__Observation	0.046	NA	NA			
macroH2A1.1 KO versus WT								
Reduced RER ~ sex + (1 timepoint) + (1 identifier)								
Full RER ~ genotype + sex + (1 timepoint) + (1 identifier)								
term	npar	AIC	BIC	logLik	deviance	statistic	f	p.value
reduced	5	-11415.087	-11384.156	5712.543	-11425.087			
full	6	-11421.323	-11384.206	5716.661	-11433.323	8.236	1	0.004
macroH2A1.2 KO versus WT								
effect	group	term	estimate	std.error	statistic			
fixed	NA	(Intercept)	0.904	0.016	56.884			
fixed	NA	genotypemutant	-0.032	0.015	-2.165			
fixed	NA	sexm	-0.050	0.015	-3.297			
random	timepoint	sd__(Intercept)	0.040	NA	NA			
random	identifier	sd__(Intercept)	0.043	NA	NA			
random	Residual	sd__Observation	0.048	NA	NA			
macroH2A1.2 KO versus WT								
Reduced RER ~ sex + (1 timepoint) + (1 identifier)								
Full RER ~ genotype + sex + (1 timepoint) + (1 identifier)								
term	npar	AIC	BIC	logLik	deviance	statistic	f	p.value
reduced	5	-6763.864	-6735.371	3386.932	-6773.864			
full	6	-6766.602	-6732.412	3389.301	-6778.602	4.739	1	0.029
macroH2A2 KO versus WT								
effect	group	term	estimate	std.error	statistic			
fixed	NA	(Intercept)	0.893	0.010	91.478			
fixed	NA	genotypemutant	0.001	0.009	0.139			
fixed	NA	sexm	-0.005	0.009	-0.573			
random	timepoint	sd__(Intercept)	0.050	NA	NA			
random	identifier	sd__(Intercept)	0.025	NA	NA			
random	Residual	sd__Observation	0.047	NA	NA			
macroH2A2 KO versus WT								
Reduced RER ~ sex + (1 timepoint) + (1 identifier)								
Full RER ~ genotype + sex + (1 timepoint) + (1 identifier)								
term	npar	AIC	BIC	logLik	deviance	statistic	f	p.value
reduced	5	-6868.379	-6839.887	3439.190	-6878.379			
full	6	-6866.400	-6832.209	3439.200	-6878.400	0.021	1	0.886

macroH2A1.1 KO versus WT (ketogenic diet)								
effect	group	term	estimate	std.error	statistic			
fixed	NA	(Intercept)	0.770	0.004	202.093			
fixed	NA	genotypemutant	-0.002	0.004	-0.472			
fixed	NA	sexm	0.008	0.004	1.853			
random	timepoint	sd__(Intercept)	0.009	NA	NA			
random	identifier	sd__(Intercept)	0.016	NA	NA			
random	Residual	sd__Observation	0.023	NA	NA			
macroH2A1.1 KO versus WT (ketogenic diet)								
Reduced RER ~ sex + (1 timepoint) + (1 identifier)								
Full RER ~ genotype + sex + (1 timepoint) + (1 identifier)								
term	npar	AIC	BIC	logLik	deviance	statistic	f	p.value
reduced	5	-17576.608	-17545.420	8793.304	-17586.608			
full	6	-17574.841	-17537.416	8793.421	-17586.841	0.233	1	0.629



Extended Data E1: Western blots showing knock-out validation (accompanying Fig. 1).

All immunoblots are shown which were used for compiling Fig. 1B. The same amount of loading was used for all runs.

Legends for Supplemental Tables S2, S5, S6

Table S2. Clinical chemistry analysis and kidney pathology results. Raw data from clinical chemistry measurements of peripheral blood from male and female macroH2A1.1 KO mice and control littermates used for the complete phenotyping. In addition, results from histopathological analysis of the kidneys are summarized. (File found separately)

Table S5. Gene ontology (GO) analysis of altered pathways in macroH2A1.1 KO liver tissue versus WT (accompanying Fig. 3). Accompanying Excel file contains complete pathway analysis with *P*-value, adjusted *P*-value, NES, size and leading edge of each pathway. (File found separately)

Table S6. Data values and statistics. All raw values contained in Figs 1 to 6 are listed if less than 20 data points per condition were acquired. Details on performed statistical test and *P*-values are found if this information was not given in the corresponding figure legend. (File found separately)